

## Ca<sup>2+</sup> buffering in the heart: Ca<sup>2+</sup> binding to and activation of cardiac myofibrils

Gerry A Smith<sup>1</sup>, Henry B F Dixon, Heide L Kirschenlohr, Andrew A Grace, James C Metcalfe and Jamie I Vandenberg

Section of Cardiovascular Biology, Department of Biochemistry, University of Cambridge, Tennis Court Rd, Cambridge CB2 1QW, UK. Tel: +44 (0)1223 333632. Fax: +44 (0)1223 333345. Email: g.a.smith@bioc.cam.ac.uk

The measurement of cardiac Ca<sup>2+</sup> transients using spectroscopic Ca<sup>2+</sup> indicators is significantly affected by the buffering properties of the indicators. The aim of the present study was to construct a model of cardiac Ca<sup>2+</sup> buffering that satisfied the kinetic constraints imposed by the maximum attainable rates of cardiac contraction and relaxation on the Ca<sup>2+</sup> dissociation rate constants and which would account for the observed effects of <sup>19</sup>F-NMR indicators on the cardiac Ca<sup>2+</sup> transient in the Langendorff-perfused ferret heart. It is generally assumed that the Ca<sup>2+</sup> dependency of myofibril activation in cardiac myocytes is mediated by a single Ca<sup>2+</sup> binding site on troponin-C. A model based on 1:1 Ca<sup>2+</sup> binding to the myofilaments, however, was unable to reproduce our experimental data, but a model in which we assumed ATP-dependent cooperative Ca<sup>2+</sup> binding to the myofilaments was able to reproduce these data. This model was used to calculate the concentration and dissociation constant of the ATP-independent myofilament Ca<sup>2+</sup> binding, giving 58 μM

and 2.0 μM respectively. In addition to reproducing our experimental data on the concentration of free Ca<sup>2+</sup> ions in the cytoplasm ([Ca<sup>2+</sup>]<sub>i</sub>), the resulting Ca<sup>2+</sup> and ATP affinities given by fitting of the model also provided good predictions of the Ca<sup>2+</sup> dependence of the myofibrillar ATPase activity measured under *in vitro* conditions. Solutions to the model also indicate that the Ca<sup>2+</sup> mobilized during each beat remains unchanged in the presence of the additional buffering load from Ca<sup>2+</sup> indicators. The new model was used to estimate the extent of perturbation of the Ca<sup>2+</sup> transient caused by different concentrations of indicators. As little as 10 μM of a Ca<sup>2+</sup> indicator with a dissociation constant of 200 nM will cause 20% reduction in peak-systolic [Ca<sup>2+</sup>]<sub>i</sub> and 30 μM will cause ≈50% reduction in the peak-systolic [Ca<sup>2+</sup>]<sub>i</sub> in a heart paced at 1.0 Hz.

### Key words:

Ca<sup>2+</sup>-transient, Troponin, Actomyosin-ATPase, Kinetics, Calcium metabolism

## Introduction

The concentration of free calcium ions in the cytoplasm ([Ca<sup>2+</sup>]<sub>i</sub>) is critical for the control of cardiac contraction (reviewed in [1]). The normal cardiac [Ca<sup>2+</sup>]<sub>i</sub> rises from a diastolic value of approx. 160 nM to a systolic value of approx. 2700 nM [2]. These values are determined by the amount of Ca<sup>2+</sup> entering and leaving the cytosol during each cardiac cycle and the kinetic properties of the cytoplasmic Ca<sup>2+</sup> buffers. Most information on cardiac [Ca<sup>2+</sup>]<sub>i</sub> has come from studies using spectroscopic Ca<sup>2+</sup> indicators (e.g. [2,3] and references therein).

These indicators can accurately report [Ca<sup>2+</sup>]<sub>i</sub> in biological tissues, but they also chelate Ca<sup>2+</sup> and therefore act as buffers [4]. Exogenous indicators, by adding to the buffering capacity, will therefore report a [Ca<sup>2+</sup>]<sub>i</sub> that may be significantly different from the unperturbed [Ca<sup>2+</sup>]<sub>i</sub>.

Endogenous Ca<sup>2+</sup> buffers in the heart may be divided into three groups based on their affinities. High affinity buffers (association constant ( $K_a$ ) > 3 × 10<sup>7</sup> M<sup>-1</sup>, e.g. calmodulin; [5]) will be >80% bound in diastole

### Abbreviations used:

ATP refers generally to the total adenosine triphosphate in the presence of at least 1 mM Mg<sup>2+</sup>, i.e. near saturated [MgATP<sup>2-</sup>];  
[Ca<sup>2+</sup>]<sub>i</sub>, concentration of free Ca<sup>2+</sup> ions in the cytoplasm;  
PCr, phosphocreatine; SOS, sum of squares;  
DiMe-5FBAPTA, 1,2-bis-[2-(1-carboxyethyl)(carboxymethyl)amino-5-fluorophenoxy]ethane;  
DiMe-4FBAPTA, 1,2-bis-[2-(1-carboxyethyl)(carboxymethyl)amino-4-fluorophenoxy]ethane;  
5FBAPTA, 1,2-bis-[2-bis(carboxymethyl)amino-5-fluorophenoxy]ethane;  
4,5FBAPTA, 1,2-bis-[2-bis(carboxymethyl)amino-4,5-difluorophenoxy]ethane;  
MFBAPTA, 1,2-bis-[2-bis(carboxymethyl)amino-5-fluoro-4-methylphenoxy]ethane.  
 $K_a$  association constant (affinity)  
 $K_d$  dissociation constant

<sup>1</sup> Address to whom correspondence should be sent

and will not contribute significantly to buffering of the cardiac  $\text{Ca}^{2+}$  transient. Conversely, buffers with low affinities (association constant  $K_a < 10^4 \text{M}^{-1}$ ) will not bind an appreciable amount of  $\text{Ca}^{2+}$  during the transient. The major contribution to cytosolic  $\text{Ca}^{2+}$  buffering during the  $\text{Ca}^{2+}$  transient will therefore be from those species with affinities in the range  $10^4$ – $10^7 \text{M}^{-1}$ . Total cardiac  $\text{Ca}^{2+}$  buffering (i.e. including high, intermediate and low affinity buffers) has been estimated from equilibrium dialysis studies to be in the range 250–300  $\mu\text{M}$  [6,7]. More recently, Bers and colleagues have estimated “fast”  $\text{Ca}^{2+}$  buffering (i.e. buffering that occurs within the time scale of the  $\text{Ca}^{2+}$  transient), assuming that  $\text{Ca}^{2+}$  buffering could be represented by a single aggregate Michaelis–Menten type species, to have a maximum binding capacity of 123  $\mu\text{M}$  with an apparent dissociation constant of 0.96  $\mu\text{M}$  [8].

The major species thought to buffer  $\text{Ca}^{2+}$  during the cardiac  $\text{Ca}^{2+}$  transient is the troponin-C component of the myofibrils [9,10]. *In vitro* studies suggest that troponin-C and intact myofibrils have only one  $\text{Ca}^{2+}$ -binding site per troponin-C with an affinity in the physiologically relevant range [11,12]. However, recent biochemical studies have shown that in the presence of ATP, the myofibrils bind  $\text{Ca}^{2+}$  cooperatively, but still only one per troponin-C, with an apparent  $K_d$  in the  $\mu\text{M}$  range [13]. In contrast with the  $\text{Ca}^{2+}$  dependency of both  $\text{Ca}^{2+}$  binding and the ATPase activity of myofibrils, the ATP dependency of the ATPase has a Hill coefficient of one. In the present study we have constructed a new model of cardiac  $\text{Ca}^{2+}$  buffering based on ATP-dependent cooperative  $\text{Ca}^{2+}$  binding to the myofilaments and used the model to calculate the affinities and concentrations of endogenous  $\text{Ca}^{2+}$  buffers and the extent of perturbation of  $\text{Ca}^{2+}$  transients that will be caused by loading  $\text{Ca}^{2+}$  indicators.

## Materials and Methods

### $^{19}\text{F}$ -NMR data base

The buffering of  $[\text{Ca}^{2+}]_i$  by  $\text{Ca}^{2+}$ -indicators is dependent on the concentration of indicator loaded and the binding affinity of the indicator. In a previous study we found that the intracellular concentration of  $^3\text{H}$ -labelled 1,2-bis-[2-bis(carboxymethyl)amino-5-fluorophenoxy]ethane (5FBAPTA) in hearts with signal-to-noise (S:N) ratio of 10:1 was approximately 120  $\mu\text{M}$  [14]. All indicators were loaded until the S:N ratio was approximately 10:1; we therefore have assumed that all indicators were present at a concentration of 120  $\mu\text{M}$  [2]. The differences in the buffering of the  $\text{Ca}^{2+}$ -transient between the different indicators will therefore predominantly reflect differences in their  $\text{Ca}^{2+}$ -affinities. The experimental determinations of diastolic and systolic  $[\text{Ca}^{2+}]_i$  in the perfused ferret heart, for indicators with  $K_d$  values ranging from 46 nM to 2950 nM are summarized in Table 1.

The data sets used in this study were acquired under two limiting sets of conditions. The  $[\text{Ca}^{2+}]$  measurements in the intact heart were obtained under isometric conditions. The ATPase measurements cited were obtained in free solution under isotonic, zero-force, conditions.

In the isometric state there is no external work performed; the ATPase continues only until sufficient cross bridges are formed to stiffen the fibres and to generate the “internal” shortening of the fibres. The experimental determinations of diastolic and systolic  $[\text{Ca}^{2+}]_i$  in the perfused heart were made under near steady-state conditions (see [2]), i.e. the rate of data block collection ( $16 \text{s}^{-1}$ ) was much slower than the rate limiting step of the isometrically limited ATPase ( $65 \text{s}^{-1}$ , see below). The rate of data collection was also rapid compared to the rise and fall of  $[\text{Ca}^{2+}]_i$  [2].

Indicator	$K_d$ at 30°C (nM)	Titration range (nM)	Indicator bound (%)	
			Diastole	Systole
4,5FBAPTA	2950	520–17,000	17	46
5FBAPTA	537	100–3,000	49	77
MFBAPTA	269	40–1,100	56	*
DiMe-4FBAPTA	155	30–900	65	82
DiMe-5FBAPTA	46	8–300	79	*

**Table 1: Summary of data for diastolic and systolic  $[\text{Ca}^{2+}]_i$  in Langendorff-perfused ferret hearts loaded with different  $^{19}\text{F}$ -NMR  $\text{Ca}^{2+}$  indicators [2].**

\* These values were not determined experimentally. They were therefore allowed to vary to make minimal direct contribution to the fitting process. However, the values obtained were included in extrapolations to obtain the unperturbed diastolic and systolic  $[\text{Ca}^{2+}]_i$  that were used to calculate the mobilized  $\text{Ca}^{2+}$  in the fitting process (see Figure 3 for details).

We have therefore used equilibrium kinetics to derive the model for  $\text{Ca}^{2+}$  buffering in the heart.

In the isotonic case there is also no external work performed; the ATPase runs until the maximal shortening is reached. The number of steps of shortening obtained per ATP consumed depends on the work done by the muscle, which is minimal when the force is zero. The ATPase data have been normalized as fractional. The removal of proportionality factors by the normalization process has allowed the use of the same equilibrium equations to generate the model predicted  $[\text{Ca}^{2+}]$  and  $[\text{ATP}]$  dependencies of the ATPase (see the Results section).

Construction of the new kinetic model of  $\text{Ca}^{2+}$ -buffering in the intact heart is based in part qualitatively on data for the  $[\text{Ca}^{2+}]$  dependence of the myofibrillar ATPase activity shown in Figure 7 of Holroyde *et al.* [11] and quantitatively on data for the  $[\text{ATP}]$  dependence of the myofibrillar ATPase activity shown in Figure 2 of Krause and Jacobus [15] (both used with permission of the authors).

### Computational methods

Solutions to the models were found by an iterative alteration of the unknown variables until the sums of squares (SOS) of the difference between the experimentally measured values and those predicted by the model were minimized, using the Microsoft Excel 98 Solver (Microsoft Corporation, Seattle, WA, USA).

The only constraints imposed were that all parameters be positive. The functions to be minimized were highly nonlinear in terms of the known variables (concentrations and affinities) therefore the quadratic extrapolation method was used to estimate the unknown variables for each one-dimensional search. Central differencing was used to refine the solutions obtained. To improve the rate of approach to solution the conjugate gradient search method was used (p. 574, Microsoft Excel Users Guide). Automatic scaling in the Excel Solver was unable to function optimally when the parameters differed by many orders of magnitude and so in this case manual scaling of the variables, by the use of log values, was also required. Where combined SOSs were used a weighting was applied so that the contribution to the solution process was the same for both sets of data.

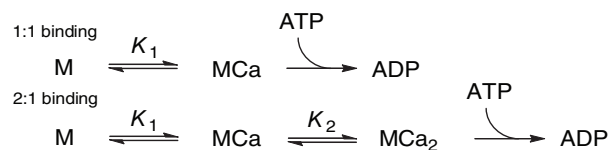
An empirical function for the variation of fraction of indicator bound to  $\text{Ca}^{2+}$  in diastole ( $[\text{FCa}]_D/[\text{F}]_T$ ) with indicator affinity ( $\log K$ ) was found by fitting those data (Table 1) to an arbitrary two term sigmoidal function,  $[\text{FCa}]_D/[\text{F}]_T = 1/(1+a^{(b-\log K)}+c^{(d-\log K)})$ , shown as solid line Figure 5. This function was then used to generate the model-derived increase in fraction bound of indicator on moving to systole as a continuous function of  $\log K$  (see Figure 3) and the expected fraction bound (dotted line Figure 5). The empirical function was used solely for presentation of the results and was not used in the fitting process.

## Results

### Inadequacies in simple models of the myofibril

#### Hill coefficient of $\text{Ca}^{2+}$ activation of the myofibrils in vitro is greater than one

The data for  $[\text{Ca}^{2+}]$ -dependence of the myofibrillar ATPase (replotted from Figure 7 of Holroyde *et al.* [11]), are shown in Figure 1. Also shown in Figure 1 are the best fits to the data for activation by 1:1 and highly cooperative 2:1 binding of  $\text{Ca}^{2+}$  to the myofibrils (dotted line and solid line respectively) based on the binding Schemes shown in Scheme 1 (below) for regulation by  $\text{Ca}^{2+}$ , in which M represents the myofibrils and  $K_1$  and  $K_2$  are the affinity constants for the first and second ions bound.



Scheme 1:

The 1:1 binding provides a very poor fit to the data, this indicates that the process exhibits cooperativity. The 2:1 model provides a much better fit, although at high  $[\text{Ca}^{2+}]$  where the data will be most accurate,

a model with more than two  $\text{Ca}^{2+}$  binding would fit better. Therefore, the myofibrillar ATPase data of Holroyde *et al.*[11] indicate that  $\text{Ca}^{2+}$  binding to the myofibrils *in vitro* is strongly cooperative so the concentration of singly ligated myofibrillar protein will be small.

#### Limitations of the 2:1 $\text{Ca}^{2+}$ binding model: the affinities of individual $\text{Ca}^{2+}$ binding steps

The pCa for half activation of the myofibrils is 6.1 (see Figure 1). In general, from product data only, it is not possible to determine the affinities of the individual binding steps. However, it is possible to impose limits on the affinities of the individual steps.

If we consider the two-step binding Scheme, then the equation for the fraction of maximal rate of reaction for the ATPase would be: (Equation 1)

$$v = V_{\max} \frac{K_1 K_2 [\text{Ca}^{2+}]^2}{1 + K_1 [\text{Ca}^{2+}] + K_1 K_2 [\text{Ca}^{2+}]^2}$$

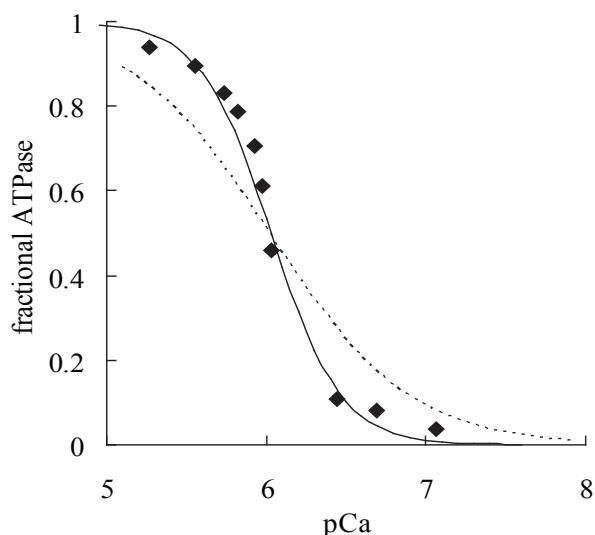


**Figure 1: Ca<sup>2+</sup> dependence of myofibrillar ATPase**

Data points (◆) are reproduced, with permission, from Holroyde *et al.* [11]. Lines represent best fits to the data for 1:1 Ca<sup>2+</sup> (dotted line) and 2:1 Ca<sup>2+</sup> (solid line) binding Schemes as described in Scheme (1) (see the text). The [Ca<sup>2+</sup>] at which the activity of the ATPase is half maximal is 10<sup>-6.1</sup>M.

where  $K_1$  and  $K_2$  represent the affinities of the two Ca<sup>2+</sup> binding steps.

If the value for the affinity of one of the binding steps (e.g.  $K_1$ ) is set, then, from any data set the corresponding value for the affinity of the other binding ( $K_2$ ) step can be found by least squares fitting. The values for  $K_2$  found for the ATPase data over a wide range of values of  $K_1$  (10<sup>3</sup>–10<sup>9</sup>M<sup>-1</sup>) and the corresponding deviations (SOSs) from ideal fit are shown in Figure 2. At values of  $K_1 > 10^5$ M<sup>-1</sup> the SOS increased significantly. This suggests that if Ca<sup>2+</sup> binding to the myofibrils follows the simple two step Ca<sup>2+</sup> binding Scheme, as described by Equation 1, then for this model  $K_1$  must be  $< 10^5$ M<sup>-1</sup> and therefore  $K_2$  must be more than 10<sup>7</sup>M<sup>-1</sup> (see Figure 2). This is not consistent with the Ca<sup>2+</sup> affinity of troponin-C (10<sup>5.6</sup>M<sup>-1</sup> e.g. [12]).

A further deficiency of this model becomes clear when account is taken of the rate at which relaxation must occur for the cardiac cycle to function at the observed maximum rate. The cardiac cycle can operate at rates up to 3–10Hz (depending on species). For a rate of 5Hz (the maximum observed for ferret; [16]) this corresponds to systolic and diastolic durations of less than 100ms each. To allow full relaxation of the myofibrils more than 95% of the second Ca<sup>2+</sup> must have dissociated from the myofibrils, i.e. the dissociation rate must be more than 50s<sup>-1</sup>. If we assume that the Ca<sup>2+</sup> on-rate for the myofibrils is maximal, i.e. limited by diffusion at  $\approx 5 \times 10^8$ M<sup>-1</sup>·s<sup>-1</sup> [17], then the upper limit

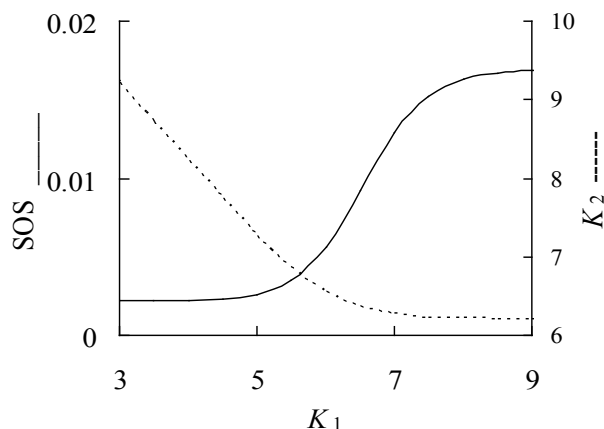


**Figure 2: Limits to the affinities for individual binding steps for the 2:1 Ca<sup>2+</sup> binding Scheme**

The effect of fixing the value for the first Ca<sup>2+</sup> affinity,  $K_1$ , in the range 10<sup>3</sup>–10<sup>9</sup>M<sup>-1</sup> for equation (2), in which the ATPase is proportional to [MCa<sub>2</sub>]. Right ordinate (broken line), the value found for  $K_2$  corresponding to each set value of  $K_1$ . Left ordinate (solid line), the SOS for the best fit to the data for values of  $K_1$ . Clearly at values of  $\log K_1 > 5$  the SOS starts to increase significantly. A very high value for  $K_1$  would ensure that the first Ca<sup>2+</sup> could not dissociate, which would make the process effectively first order, already shown to give a very poor fit to the data (Figure 1).

for the affinity of the second Ca<sup>2+</sup> binding step ( $K_2$ ) would be  $5 \times 10^8 / 50$ , i.e. 10<sup>7</sup>M<sup>-1</sup>. In practice the high protein concentration makes the diffusion rate in the cytosol considerably less than that in water. Therefore, the data fitting, shown in Figure 2, indicating that  $K_2$  must be considerably greater than 10<sup>7</sup>M<sup>-1</sup>, is not compatible with the kinetic constraints of the rates of contraction and relaxation of the myofibrils. This means that Ca<sup>2+</sup> binding to the myofibrils cannot be explained by the simple two-step binding process described in Equation 1. By analogous reasoning Ca<sup>2+</sup> binding to the myofibrils cannot be explained by a third or higher order allosteric regulated binding Scheme. Therefore, given that Ca<sup>2+</sup> binding to the myofibrils is cooperative (see Figure 1), Ca<sup>2+</sup> binding to the myofibrils must be modulated by other factors.

#### *Limitations of the 2:1 Ca<sup>2+</sup> binding model: the Hill coefficient for ATP activation of the myofibrillar ATPase is unity*

It has previously been proposed that cooperativity between cross-bridges could explain the high Hill coefficient of the [Ca<sup>2+</sup>] activation of the ATPase. This would be equivalent to M (in Scheme 1) being two separate enzyme units both binding Ca<sup>2+</sup> and ATP and working in concert. This mechanism is inconsistent with the lack of cooperativity seen for the [ATP] dependency of the ATPase (see the Discussion section). In addition, the limits to Ca<sup>2+</sup> affinity set by the maximum cardiac rate would also apply for this model.

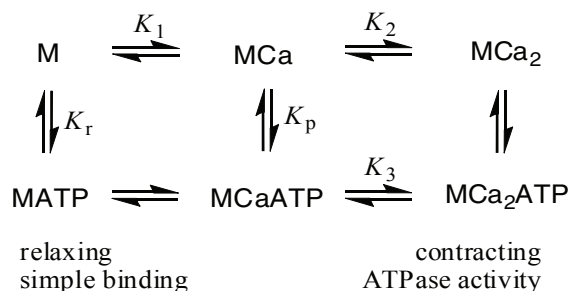
## Resolution of the simple model problems

### Modulation of $Ca^{2+}$ binding by ATP

The obvious candidate for modulation of  $Ca^{2+}$  binding to the myofibrils is ATP, the substrate for the ATPase. Taylor and Weeds [18] have shown that the rate limiting step of the myofibrillar ATPase was the rate of ADP dissociation which has a rate constant of  $65s^{-1}$ . The similarity of the rate of ATP hydrolysis with the minimum constraint imposed by the rate of relaxation ( $50s^{-1}$ , see above) suggests that it may be the rate of ATP hydrolysis that limits the rate of relaxation. If binding a second  $Ca^{2+}$  depended on ATP, e.g. the affinity were high in the presence of bound ATP (low dissociation rate) but low in the absence of bound ATP (fast dissociation rate), then the effective  $Ca^{2+}$  dissociation rate would approach that of the ADP dissociation rate, i.e.  $65s^{-1}$ . In effect, the affinity of the  $Ca^{2+}$  binding could be much greater than  $10^7M^{-1}$  in the presence of bound ATP, yet still have an effective dissociation rate of  $\approx 50s^{-1}$ .

Recent  $^{45}Ca$  binding studies have shown that in the presence of ATP,  $Ca^{2+}$  binding to the myofibrils has increased cooperativity [13,19], which is consistent with ATP-dependence of the  $Ca^{2+}$  binding. However, it is not possible to determine from the data of [13] the exact degree of cooperativity in the presence of ATP because of the inaccuracies in determining the Hill coefficient of  $Ca^{2+}$  binding and the possibility of diffusion-limited control of local ATP levels within myofibrils as seen during ATPase measurements. In addition to  $Ca^{2+}$  binding being ATP dependent (see above), Arata *et al.* [20] have shown that in the presence of low  $[Ca^{2+}]$ , ATP inhibits contractility indicating that there is substrate inhibition. This substrate inhibition suggests that there is a degree of ordered binding of the  $Ca^{2+}$  and ATP to the myofibrils.

The simplest model that can explain the cooperative  $[Ca^{2+}]$  data of Holroyde *et al.* [11], and the ATP dependency of  $Ca^{2+}$  binding shown by Morimoto and Ohtsuki [13] and Tobacman [19] is illustrated by steps  $K_1$ ,  $K_p$  and  $K_3$  in Scheme 2. This we shall refer to as the Ca-ATP-Ca model.



(Scheme 2: )

### Scheme 2: Ca-ATP-Ca model of $Ca^{2+}$ and ATP binding to the myofibrils

The simplest model based on the ATP-dependent cooperative  $Ca^{2+}$ -binding observed by Morimoto and Ohtsuki [13] is represented by the following steps;  $K_1$ , The  $Ca^{2+}$ -free myofilament (M) binds the first  $Ca^{2+}$  ion;  $K_p$ , the myofilament with one bound  $Ca^{2+}$  binds ATP;  $K_3$ , a second  $Ca^{2+}$  is bound. The cooperativity of  $Ca^{2+}$ -binding requires  $K_3 > K_1 > (K_2)/4$  resulting in a strongly bound ATP state generating the ATPase activity. The full Scheme incorporates the pre ATP binding of the second calcium ( $K_2$ ) which is required to give the limiting value for ATP apparent affinity at high  $[Ca^{2+}]$ . Effectively the affinity of the second  $Ca^{2+}$  binding ( $K_2$ ) is increased (to  $K_3$ ) by the prior binding of ATP. Also included is the  $Ca^{2+}$ -independent ATP binding ( $K_r$ ) which has been equated to the "loosely bound ATP state" and results in relaxation of the protein.

### Additional features incorporated into the new kinetic model of $Ca^{2+}$ binding

In addition to the basic Scheme ( $K_1-K_p-K_3$ ) illustrated in Scheme 2, we have incorporated additional features into the new kinetic model of  $Ca^{2+}$  binding to the myofibrils based on the following observations:

1. The apparent ATP affinity of the myofibrillar ATPase approaches a high limiting value when the  $[Ca^{2+}]$  is increased [15]. The ATP-induced  $Ca^{2+}$ -binding cooperativity [19] implies ATP binding before the second  $Ca^{2+}$ . The Scheme allows a second  $Ca^{2+}$  to bind before ATP ( $K_2$ , in Scheme 2), as well as after ATP ( $K_3$ ). For this Scheme the apparent ATP affinity at very high  $[Ca^{2+}]$  will be  $K_p \cdot K_3 / K_2$ . Without the ATP-independent  $Ca^{2+}$  binding, i.e. if  $K_2$  were to be zero, the apparent affinity for ATP would increase indefinitely with  $[Ca^{2+}]$ .
2. The myofibrils can bind ATP in the absence of  $Ca^{2+}$  ( $K_r$ , in Figure 3), termed the loose-bound ATP state [21]. The value of  $K_r$ , measured from the ATP-dependent changes in fluorescence of the isolated myofibrils is  $\approx 10^3M^{-1}$  [18,21]. The substrate inhibition shown by Arata *et al.* [20] could arise from this binding.

### Summary of the model of $Ca^{2+}$ binding

In summary, the studies of Holroyde *et al.* [11], Tobacman [19] and Morimoto and Ohtsuki [13] indicate that  $Ca^{2+}$  binding to the myofibrils is cooperative and ATP-dependent. A complete description of  $Ca^{2+}$  binding to the myofibrils must also take into account the possibility that two  $Ca^{2+}$  can bind without ATP [19] and that ATP can bind with or without one or both  $Ca^{2+}$  [21] (Scheme 2).

## Derivation of a new kinetic model of Ca<sup>2+</sup> buffering in the intact heart

(Equation 5)

Although the myofibrils represent the major source of Ca<sup>2+</sup> binding during the cardiac Ca<sup>2+</sup> transient, any model of Ca<sup>2+</sup> buffering in the intact heart must also consider the contributions of other endogenous buffers and any exogenous buffers (e.g. Ca<sup>2+</sup> indicators loaded into the heart). Furthermore to calculate the buffering of Ca<sup>2+</sup> in the intact heart it is also necessary to know how much Ca<sup>2+</sup> enters the cytoplasm (from extracellular as well as intracellular stores) during each contraction.

### Ca<sup>2+</sup> binding to the myofibrils

From the mass action equations applicable to Scheme 2 an expression can be derived for the total concentration of myofibrils, [M]<sub>T</sub>: (Equation 2)

$$[M]_T = [M] \left( \frac{1 + K_1 [Ca^{2+}] + K_r [ATP] + K_p [ATP] [Ca^{2+}]}{+ K_2 [Ca^{2+}]^2 + K_3 [Ca^{2+}] [ATP] [Ca^{2+}]^2} \right)$$

where  $K_1$ ,  $K_2$ ,  $K_3$  and  $K_r$ ,  $K_p$  are the affinity constants for the myofibrillar Ca<sup>2+</sup> binding and the myofibrillar ATP binding (see Scheme 2) and [M]<sub>T</sub>, [M] are the concentration of total myofilaments and free myofilaments.

Because we are studying Ca<sup>2+</sup>-dependency, it is convenient to have [Ca<sup>2+</sup>] as the sole variable and treat [ATP] as a parameter, so that the equation may be simplified to; (Equation 3)

$$[M]_T = M \left( \alpha + \beta [Ca^{2+}] + \gamma [Ca^{2+}]^2 \right) \quad \text{where} \quad \begin{aligned} \alpha &= 1 + K_1 [ATP] \\ \beta &= K_1 + K_2 K_p [ATP] \\ \gamma &= K_1 (K_2 + K_3 K_p [ATP]) \end{aligned}$$

and hence we can obtain an expression for the fraction of the myofibrils activated as M<sub>Ca<sub>2</sub>ATP</sub>, denoted  $Q$ , which for the case of the Ca-ATP-Ca model (Scheme 2) is: (Equation 4)

$$Q = \frac{K_1 K_3 K_p [ATP] [Ca^{2+}]^2}{\alpha + \beta [Ca^{2+}] + \gamma [Ca^{2+}]^2}$$

### Ca<sup>2+</sup> binding to other endogenous Ca<sup>2+</sup> buffers

Other non-myofibrillar Ca<sup>2+</sup> binding species, e.g. calmodulin and proteins on the cytoplasmic leaflets of both the sarcolemma and the sarcoplasmic reticulum membranes [9,10], may also contribute to Ca<sup>2+</sup>-buffering in the intact heart. If we assume that the additional endogenous Ca<sup>2+</sup> buffers can be considered as a single species that binds one Ca<sup>2+</sup> ion, then the following expression for the total calcium, [Ca]<sub>T</sub>, in the cytoplasm can be derived:

$$[Ca]_T = [Ca^{2+}] + [M]_T \frac{(\beta [Ca^{2+}] + 2\gamma [Ca^{2+}]^2)}{(\alpha + \beta [Ca^{2+}] + \gamma [Ca^{2+}]^2)} + [E]_T \frac{K_E [Ca^{2+}]}{(1 + K_E [Ca^{2+}])}$$

where [E]<sub>T</sub> is the total amount of other endogenous buffers attributed an affinity constant of  $K_E$ .

As the 1:1 endogenous buffers would reduce the effective Hill coefficient of the cytosolic buffering similar equations have also been derived for models where the additional endogenous Ca<sup>2+</sup> buffers bind Ca<sup>2+</sup> cooperatively (see the Discussion section).

### Ca<sup>2+</sup> binding to exogenous Ca<sup>2+</sup> buffers (Ca<sup>2+</sup> indicators)

To calculate Ca<sup>2+</sup> buffering in the presence of Ca<sup>2+</sup> indicators we measure the change in the fraction of indicator bound to Ca<sup>2+</sup> between diastole and systole [2],  $\Delta[FCa]/[F]_T$ , i.e.: (Equation 6)

$$\Delta[FCa]/[F]_T = \left( \frac{[FCa]_S}{[F]_T} - \frac{[FCa]_D}{[F]_T} \right)$$

where [FCa] and [F]<sub>T</sub> are the concentrations of Ca<sup>2+</sup> bound and total indicator. The subscripts S and D refer to systole and diastole.

### Ca<sup>2+</sup> entry into the cytoplasm during the Ca<sup>2+</sup> transient

To calculate the buffering of [Ca<sup>2+</sup>]<sub>i</sub> in the intact heart it is necessary to know how much Ca<sup>2+</sup> enters the cytoplasm ( $\Delta[Ca]_T$ ) as well as the change in [Ca<sup>2+</sup>]<sub>i</sub> during each contraction. For the purposes of the model it is assumed that all sources of Ca<sup>2+</sup> entry (from extracellular as well as intracellular sources) can be combined into a single Ca<sup>2+</sup> source. As a first approximation we have assumed that the total Ca<sup>2+</sup> mobilized during the cardiac cycle is independent of total (endogenous + exogenous) cytosolic Ca<sup>2+</sup> buffering (see Discussion).  $\Delta[Ca]_T$  can then be calculated as the sum of the changes in [Ca<sup>2+</sup>]<sub>i</sub>, Ca<sup>2+</sup> bound to the myofibrils, Ca<sup>2+</sup> bound to other endogenous buffers, and Ca<sup>2+</sup> bound to the indicator, between diastole and systole: (Equation 7)

$$\Delta[Ca]_T = \left\{ \begin{aligned} & [Ca^{2+}]_S - [Ca^{2+}]_D + (\sum [MCA]_S - \sum [MCA]_D) \\ & + 2(\sum [MCA_2]_S - \sum [MCA_2]_D) + ([ECa]_S - [ECa]_D) + \Delta[FCa] \end{aligned} \right\}$$

The  $\sum$  terms are used to indicate all species that are bound to either one or two Ca<sup>2+</sup> with or without ATP (see Scheme 2).

Substitutions can be made to reduce this equation to a function of the known or measurable variables and parameters: [Ca<sup>2+</sup>], [ATP] and  $K_p$ , and the seven unknowns, viz.  $\Delta[Ca]_T$ , [M]<sub>T</sub>, [E]<sub>T</sub>,  $K_1$ ,  $K_2$ ,  $K_3$  and  $K_p$

which can be expressed as a function of the measured variable, the change in fraction of indicator bound to  $\text{Ca}^{2+}$ ,  $\Delta[\text{FCa}]/[\text{F}]_{\text{T}}$ : (see Equation 8)

This equation therefore represents the new kinetic model of  $\text{Ca}^{2+}$  buffering in the intact heart that we have used to fit the NMR data for indicator  $K_d$ -dependent decline in  $[\text{Ca}^{2+}]_i$  and thereby to estimate parameters for  $\text{Ca}^{2+}$  binding to the myofibrils and other endogenous  $\text{Ca}^{2+}$  buffers in the heart.

$$\Delta \frac{[\text{FCa}]}{[\text{F}]_{\text{T}}} = \left( \frac{\frac{\Delta[\text{Ca}]_{\text{T}} - [\text{Ca}^{2+}]_{\text{S}}}{[\text{F}]_{\text{T}}} \left\{ 1 + \frac{[\text{M}]_{\text{T}}(\beta + 2\gamma[\text{Ca}^{2+}]_{\text{S}})}{(\alpha + \beta[\text{Ca}^{2+}]_{\text{S}} + \gamma[\text{Ca}^{2+}]_{\text{S}}^2)} + \frac{[\text{E}]_{\text{T}}K_{\text{E}}[\text{Ca}^{2+}]_{\text{S}}}{(1 + K_{\text{E}}[\text{Ca}^{2+}]_{\text{S}})} \right\}}{+ [\text{Ca}^{2+}]_{\text{D}} \frac{[\text{M}]_{\text{T}}(\beta + 2\gamma[\text{Ca}^{2+}]_{\text{D}})}{[\text{F}]_{\text{T}}} \left\{ 1 + \frac{[\text{M}]_{\text{T}}(\beta + 2\gamma[\text{Ca}^{2+}]_{\text{D}})}{(\alpha + \beta[\text{Ca}^{2+}]_{\text{D}} + \gamma[\text{Ca}^{2+}]_{\text{D}}^2)} + \frac{[\text{E}]_{\text{T}}K_{\text{E}}[\text{Ca}^{2+}]_{\text{D}}}{(1 + K_{\text{E}}[\text{Ca}^{2+}]_{\text{D}})} \right\}} \right)$$

## Constraining the kinetic model of $\text{Ca}^{2+}$ buffering in the intact heart to fit the experimental data

To determine the parameters for  $\text{Ca}^{2+}$  buffering in the intact heart we constrained the model to fit two independent sets of results: first, the changes in the  $\text{Ca}^{2+}$ -transient following the loading of  $^{19}\text{F}$ -NMR  $\text{Ca}^{2+}$  indicators in the Langendorff-perfused ferret heart [2] and second, the [ATP] dependence of the myofibril ATPase activity [15].

### ATPase is treated as measured under equilibrium conditions

In the heart the ATP hydrolysis step is rendered essentially irreversible by the very low  $[\text{P}_i]$  maintained by the phosphate pumping of the mitochondria. The ATPase measurements are initial rates and may also be considered irreversible. In the derivation of the model the equilibrium equations were for the isometric condition where the total ATPase turnover is limited by steric constraints and hence time is available for equilibrium of the species of Scheme 2 to be reached.

For the isolated ATPase measurements the near equilibrium condition may not hold in the steady state. The rate limiting step returns the myofibril, presumably with one or two  $\text{Ca}^{2+}$  bound, to the active pool. The prerequisite for the maximum possible rate of relaxation of the myofibrils is that the dissociation rates of the  $\text{Ca}^{2+}$  binding steps ( $K_1$  and  $K_2$ ), and consequently any subsequent ATP binding, must be faster than  $50\text{s}^{-1}$ . This minimum rate is close to the rate-limiting ADP dissociation rate. Therefore, for the Ca-ATP-Ca model, these steps will approach equilibrium in the steady state. Thus, any appreciable displacement from equilibrium will result only from the relative rates of formation and dissociation of the  $\text{MCA}_2\text{ATP}$  species and the loss of this species by the rate limiting ADP dissociation. However, in the steady state the concentration of  $\text{MCA}_2\text{ATP}$  will be proportional to its rate of formation, i.e. the concentration of the precursor ( $\text{MCAATP}$ ) multiplied by the  $[\text{Ca}^{2+}]$  and a constant. If normalized rates (fraction of maximal ATPase) are used then the constant disappears from the numerator of Equation 4. The rate limiting step returns the myofibril to the pool equilibrating with  $\text{Ca}^{2+}$  and ATP

bound species and is included as  $\text{MCA}_2\text{ATP}$  in the sum of species making up the total myofibril concentration in the denominator of Equation 4. Therefore, with the above considerations we may use Equation 4 for the derivation of normalized ATPase rates.

To test the validity of using the equilibrium equations for the ATPase in the model, we have multiplied by a factor the value of  $[\text{MCA}_2\text{ATP}]$  predicted by assuming equilibrium. The closeness of fitting the combined NMR and [ATP] data was critically dependent on this factor which approached unity when allowed to vary during the solution process, (more than 0.95, dependent on stringency).

### Limits for the second ATP-independent $\text{Ca}^{2+}$ -binding strength

In the physiological range of  $[\text{Ca}^{2+}]$ , the  $\text{Ca}^{2+}$  binding to myofibrils measured in the absence of ATP appears to be one per troponin unit and is clearly not positively cooperative [13] which would seem to be at odds with the model derived above, unless  $K_2 \ll K_1$  and not titrated in the range of  $[\text{Ca}^{2+}]$  studied. However, if M in the equations refers to more than one unit then for the two-sub unit case where there is no positive cooperativity,  $K_2$  cannot exceed  $K_1/4$  (the result of two independent sites with affinity  $K_1/2$ ). Higher order multimers would result in a greater separation of the observed affinities. We have therefore applied the minimal constraint  $K_2 < K_1/4$ .

The change in the amount of indicator bound to  $\text{Ca}^{2+}$  between diastole and systole for the five indicators (Table 1) is shown in Figure 3 (◆) and the data for the [ATP] dependence of the ATPase obtained by Krause and Jacobus [15] are shown in Figure 4 (■). Constraining the model to fit the  $\text{Ca}^{2+}$  binding data from the NMR experiments alone does not enable us to calculate the affinities  $K_1$ ,  $K_2$ ,  $K_3$  and  $K_p$  unless we also specify the [ATP] dependence of  $\text{Ca}^{2+}$  binding to the myofibrils. This was achieved by simultaneously fitting the data in Table 1 and those from Krause and Jacobus by iteration of the variables in Equations 8 and 4, respectively, to minimize the combined SOS for both fits.

This effectively constrains the apparent ATP dissociation constant of the myofilaments to  $13.6\mu\text{M}$ , when  $\text{pCa}=4.5$ , as measured by Krause and Jacobus [15]. The line in Figure 3 shows the best fit of the Ca–ATP–Ca model to the NMR data and the line in Figure 4 the associated fit to the ATPase against [ATP].

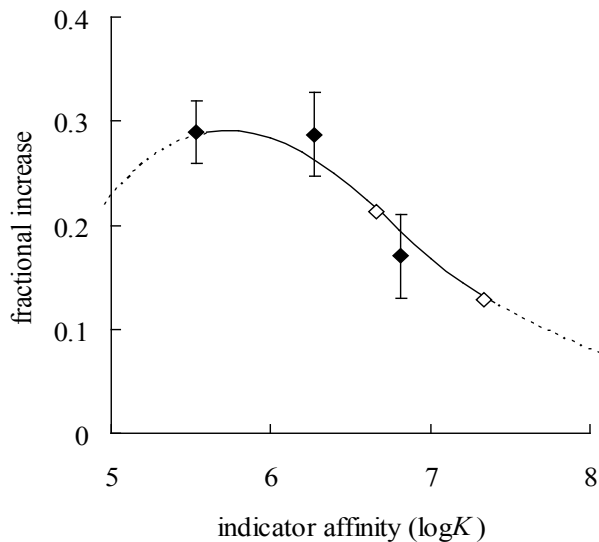


**Figure 3: The increase between diastole and systole in the fraction of  $^{19}\text{F}$  indicator that is  $\text{Ca}^{2+}$  bound**

The changes observed are shown (■). The line represents best fit for the Ca–ATP–Ca model. Values for the systolic  $[\text{Ca}^{2+}]_i$  in the presence of 1,2-bis-[2-bis(carboxymethyl)amino-5-fluoro-4-methylphenoxy]ethane (MFBAPTA) and 1,2-bis-[2-(1-carboxyethyl)(carboxymethyl)amino-4-fluoro-phenoxy]ethane (DiMe-4FBAPTA) (◇) were allowed to vary, because there were no experimental measurements of these values, and so they made no contribution to the sum of squares calculations. Values for the systolic  $[\text{Ca}^{2+}]_i$  for all indicators, however, were included in the extrapolation process to determine the unperturbed systolic and diastolic  $[\text{Ca}^{2+}]_i$  in each model solution. In all cases the values for unperturbed diastolic and systolic  $[\text{Ca}^{2+}]_i$  for the best fits of the models were in the range  $150\pm 10\text{nM}$  and  $2670\pm 50\text{nM}$  respectively. Both values are very similar to those we obtained in the accompanying paper [2]. The best fit shown for the Ca–ATP–Ca model was obtained by simultaneously constraining the model to fit both the NMR data and the [ATP] dependence of the ATPase (see Figure 4). The fractional increases calculated are for the point measurements only. A continuous function for the increase between diastole and systole was derived as detailed in computational methods and Figure 5. Outside the range of indicator affinities used the continuous function is unreliable, therefore, the resultant curve is plotted as dotted line in these regions. However, as expected the increase tends to zero each side of the data range available.

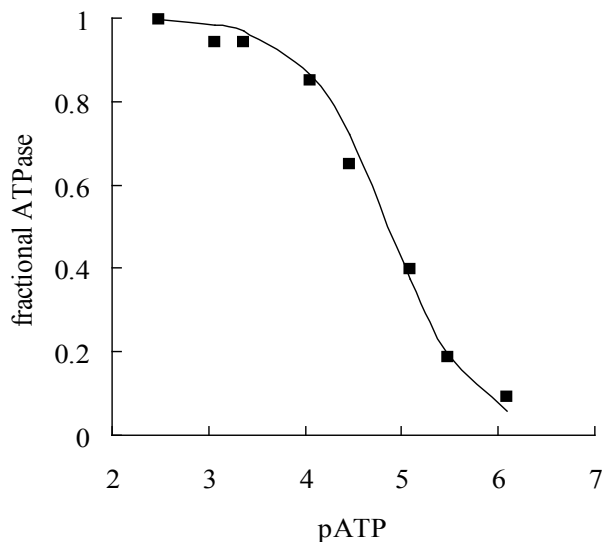


**Figure 4: Constraining the models to the [ATP] against ATPase data**

Data for the [ATP] dependence of the myofibrillar ATPase in the presence of PCr (■) (re-plotted from Krause and Jacobus [15] with the permission of the authors). The line of best fit was calculated from the Ca–ATP–Ca model. The SOS of the errors between the model calculated values (solid line) and the experimental values (■) for the ATPase were combined with the SOS derived from the NMR data (shown in Figure 3). Scaling was applied so that each set of SOS would make approximately equal contribution to the final SOS. The best fits shown in both Figure 3 and 4 were thence obtained by minimising the combined SOS.

The derivation of a continuous function for the best fit to the NMR data is given in the Computational Methods section and Figure 5.

The data fitting of the Ca–ATP–Ca model shown in Figures 3 and 4 yields values for the  $\text{Ca}^{2+}$ -affinities,  $K_p$ ,  $K_3$  and the product  $K_3K_p$  (see below). It is not possible to determine separate values for the affinities  $K_3$  and  $K_p$  as only data on the concentration of end product are available. In practice the constants  $K_3$  and  $K_p$  were allowed to vary independently in the model but we only report values for the product  $K_3K_p$ . The fitting also gives values for the concentration of myofibrils  $[\text{M}]_T$ , the amount of calcium released during the transient  $\Delta[\text{Ca}]_T$  and sets limits on the parameters of other endogenous buffers. The model-derived parameters can be used to predict the effect of loading any concentration of any  $\text{Ca}^{2+}$ -indicator on the cardiac  $\text{Ca}^{2+}$  transient.

In addition to the fitting of the empirical function to the diastolic NMR results, Figure 5 also shows the correlation of the derived systolic NMR data with those observed.

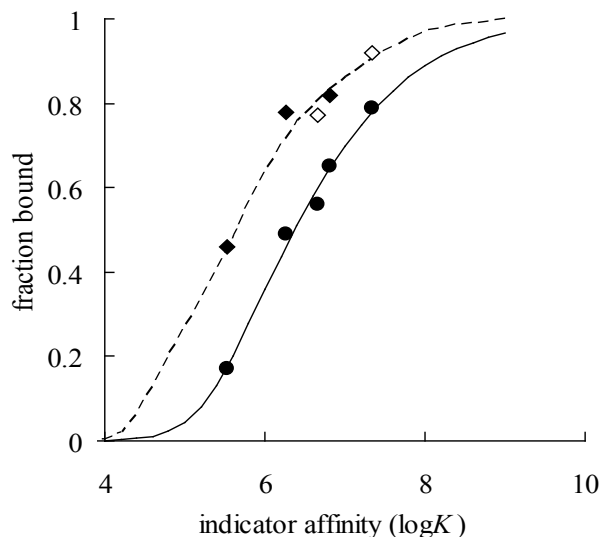


**Figure 5:**

**Derivation of continuous functions for fraction of indicator bound to  $\text{Ca}^{2+}$  plotted against indicator  $K_d$**

The data from Table 1 are shown [diastolic ( $\bullet$ ) and systolic ( $\blacklozenge$ )]. The solid line is the best fit of the arbitrary two term sigmoidal function,  $[\text{Fca}]_D/[\text{F}]_T = 1/(1+a^{(b-\log K)}+c^{(d-\log K)})$ , to the diastolic data. The constants derived were  $a=3.4213$ ,  $b=6.3056$ ,  $c=51.1540$ ,  $d=5.7185$ . This function was not used in the fitting of the Ca-ATP-Ca model to the experimental data. The broken line represents the expected systolic fraction bound calculated from the diastole fitted curve using the constants derived from the model fitting. However, the difference between the two curves was used to show the result of the model fitting in Figure 3.

**Values for the concentration and affinities of  $\text{Ca}^{2+}$  buffers in the intact heart derived from the new kinetic model of  $\text{Ca}^{2+}$  buffering**

*Concentration and affinity of myofibrillar  $\text{Ca}^{2+}$  binding sites*

For the Ca-ATP-Ca model the data fitting fully utilized the constraint based on the interaction of two myofibrillar sub units, i.e. M has two troponin sites. The predicted affinities of the first and second ATP-independent  $\text{Ca}^{2+}$  binding were  $10^6$  and  $10^{5.4}\text{M}^{-1}$  respectively. The apparent dissociation constant for the myofibrillar  $\text{Ca}^{2+}$  binding was 580nM (in the presence of saturating phosphocreatine (PCr) and 5mM ATP) and the concentration of  $\text{Ca}^{2+}$  binding sites was  $2 \times 29 = 58\mu\text{M}$ . The total mobilized  $\text{Ca}^{2+}$ ,  $\Delta[\text{Ca}]_T$ , was  $44\mu\text{M}$ . The value for  $\log(K_3K_p)$ , the ATP and subsequent  $\text{Ca}^{2+}$  binding step, was 10.6. During low stringency fitting the value of  $K_p$  rapidly approached  $10^{8.5}$  and increased to very high values as the stringency was increased.

In addition, if the two ATP-independent  $\text{Ca}^{2+}$ -binding steps ( $K_1$  and  $K_2$ ) are replaced in the solution process with two non-interacting binding sites, i.e. using group constants without any constraint applied, these sites are found to be identical with a concentration of  $29\mu\text{M}$  and an affinity of  $10^{5.7}\text{M}^{-1}$ .

*Comparison of the model predicted and in vitro measurements of the  $[\text{Ca}^{2+}]$  dependence of the myofibrillar ATPase*

Our model was constrained to fit data obtained under *in vivo* conditions, i.e. in the presence of saturating PCr and  $[\text{ATP}] = 5\text{mM}$  [22]. The *in vitro* data, obtained by Holroyde *et al.* [11] for the  $\text{Ca}^{2+}$  dependence of the ATPase, however, were obtained in the absence of PCr and with  $[\text{ATP}] = 3\text{mM}$ . Krause and Jacobus [15] showed that the  $[\text{ATP}]$  dependence of the ATPase is dependent on PCr. At  $\text{pCa} = 4.5$  the  $[\text{ATP}]$  required for half activation of the myofibrils

$[Q = 0.5$ , Equation 4] was a minimal  $13.6\mu\text{M}$  in the presence of saturating PCr and  $79.9\mu\text{M}$  in the absence of PCr. The value obtained for  $K_3K_p$  depends on this apparent ATP affinity [see Equation 4]. Therefore, to reproduce the  $\text{Ca}^{2+}$  dependence of the ATPase under conditions *in vitro* we recalculated  $K_3K_p$  for the absence of PCr. In addition to the absence of PCr the data of Holroyde *et al.* [11] were obtained at  $4\text{mM}$   $[\text{Mg}^{2+}]$  whereas under the conditions of the NMR experiments (and therefore in our model) the  $[\text{Mg}^{2+}]_i$  is  $1.2\text{mM}$  [23]. It has been shown that the apparent affinity of the ATPase for  $\text{Ca}^{2+}$  is  $[\text{Mg}^{2+}]$  dependent; a five-fold increase in the  $[\text{Mg}^{2+}]$  from 2 to  $10\text{mM}$  causes a 0.38 pCa shift in the apparent  $K_d$  for  $\text{Ca}^{2+}$  of the ATPase [24]. Therefore, assuming the apparent  $\text{Ca}^{2+}$  dissociation constant has linear dependence on  $[\text{Mg}^{2+}]$  over the range 1 to  $10\text{mM}$ , we have generated values for the data of Holroyde *et al.* [11] that would be expected at  $1.2\text{mM}$   $\text{Mg}^{2+}$ , by adding 0.3 to their pCa values.

The data for the  $\text{Ca}^{2+}$  dependence of the myofibrillar ATPase under conditions *in vitro*, as above, is plotted in Figure 6 (page II-10) ( $\blacklozenge$ ) along with the  $\text{Ca}^{2+}$  dependence of the myofibrillar ATPase predicted by the Ca-ATP-Ca model (solid line) as fitted to the NMR data (Table 1) and the  $[\text{ATP}]$  dependence data of Krause and Jacobus [15].

*Additional endogenous buffers*

For the Ca-ATP-Ca model the predicted affinity and/or concentration of the additional endogenous buffer,  $K_E$  and  $[\text{E}]_T$ , are too low to make any significant contribution to  $\text{Ca}^{2+}$ -buffering. These results rule out other endogenous non-cooperative cytosolic  $\text{Ca}^{2+}$  buffers contributing to buffering of the cardiac

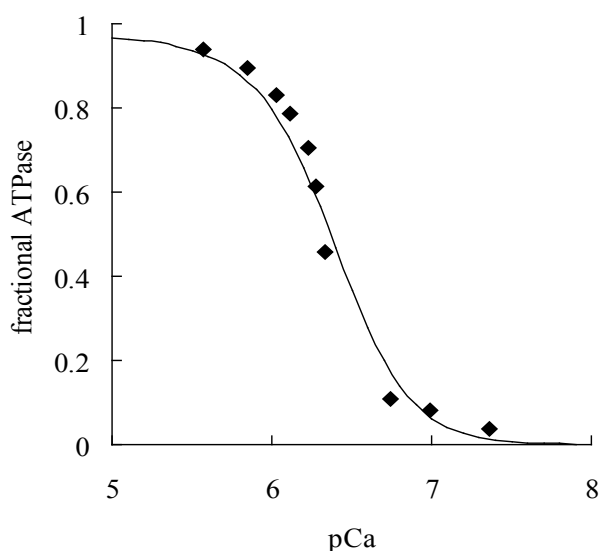


**Figure 6: Model predicted values for  $[Ca^{2+}]$  dependency of the myofibrillar ATPase**

Comparison of the values calculated from the Ca-ATP-Ca model for the  $[Ca^{2+}]$  dependency of the myofibrillar ATPase activity (solid line) and the experimental data obtained by Holroyde *et al.* (◆) [11] corrected to that expected for a  $[Mg^{2+}]$  of 1.2mM (see text for details).

$Ca^{2+}$  transient. However, if the additional buffer was cooperative with two sites for  $Ca^{2+}$  with an apparent dissociation constant close to that of the myofibrils, this buffer could be included in the total binding sites of  $58\mu M$  with the myofibrils making up one component and the additional buffer the remainder. It is not possible within the limits of the experimental errors of our NMR measurements to determine if the buffering is composed of a single component or two components with similar characteristics. Solutions to the data fitting when an additional buffer with cooperative binding is included do show minimization of the sum of squares as its concentration approaches zero, albeit with a very small gradient of approach to minimum (Figure 7).

#### Effect of the indicator concentration on the $Ca^{2+}$ transient

To obtain adequate S:N ratios,  $^{19}F$ -NMR indicators have to be loaded to concentrations of approx.  $120\mu M$ , which clearly perturbs the  $[Ca^{2+}]$  transient [2]. We can use the model to calculate the perturbation of the  $Ca^{2+}$  transient that would occur for any  $Ca^{2+}$  indicator at any concentration. Figure 8 shows the predicted effect of loading an indicator with a  $K_d$  value of 220nM at intra-cellular concentrations of 0–250mM. The model predicts that even at  $30\mu M$  an indicator with  $K_d=220nM$  would reduce the  $[Ca^{2+}]$  transient by approx. 50%. It is noted that Figure 8 reflects the time course of developed pressure found when loading indicators into the heart reflecting a constant rate of hydrolysis of the acetoxymethyl esters in the cytosol [25–27].

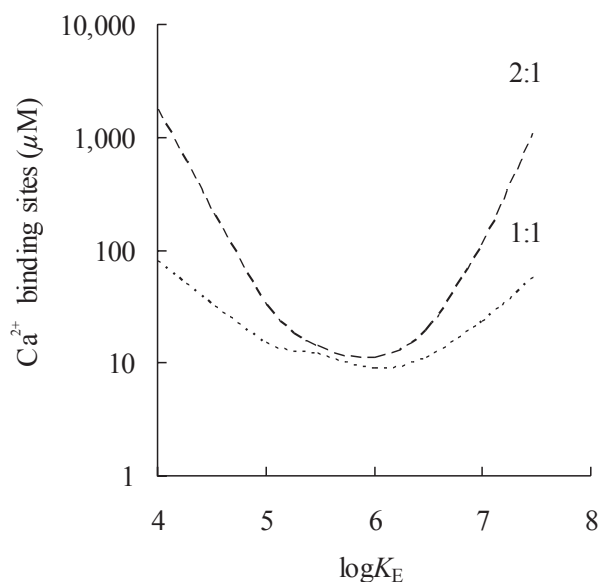


**Figure 7: Additional endogenous buffers**

The solution process for the Ca-ATP-Ca model resulted in a fit of the data that was just within the random experimental error. This allows for little or no additional endogenous buffering. If we assume a cumulative error resulting from approximations made then a limit to the other endogenous buffers can be estimated as follows; The solution results are taken as correct within the context of the accumulated error; the additional buffering that can be added keeping the solution to these values within the random experimental error may then be estimated. Shown are the maximum extra 1:1 (dotted line) or 2:1 (broken line) endogenous  $Ca^{2+}$  buffer concentrations as a function of their affinities that can be added using this approach.

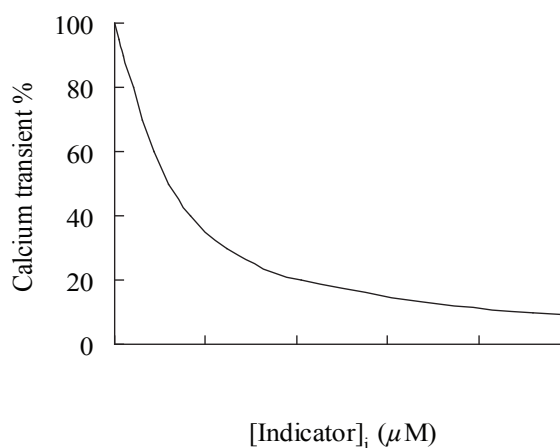


**Figure 8: Effect of  $Ca^{2+}$  indicators on cardiac  $Ca^{2+}$  transients**

The expected  $[Ca^{2+}]_i$  transients in ferret heart loaded with varying concentrations of indicator with  $K_d$  of 220nM. It was assumed that diastolic  $[Ca^{2+}]_i$  rises asymptotically to a raised value at high indicator concentrations such that the diastolic  $[Ca^{2+}]_i$  at  $120\mu M$  indicator was the same as that measured experimentally (see Table 1).

## Discussion

### A new kinetic model of Ca<sup>2+</sup>-buffering in the intact heart

Previous estimates of Ca<sup>2+</sup> buffering in the heart have usually assumed that it is composed of one or more buffer species each with a single site for Ca<sup>2+</sup> (e.g. [7,28]). These models could not reproduce our <sup>19</sup>F-NMR data (Figure 3). However, our re-analysis of the data *in vitro* for the [Ca<sup>2+</sup>] dependence of the myofibrillar ATPase showed that Ca<sup>2+</sup> binding to the myofibrils (the most significant source of Ca<sup>2+</sup> buffering in the heart; [10]), must bind at least two Ca<sup>2+</sup> ions cooperatively (see Figure 1). We used this observation as the basis for the new model of Ca<sup>2+</sup> buffering in the intact heart. In formulating the model we have also taken into account the constraints imposed by the kinetics of cardiac contraction which dictate that the rates of dissociation of Ca<sup>2+</sup> from the myofibrils must be at least 50s<sup>-1</sup> and that Ca<sup>2+</sup> binding to the myofibrils must be ATP-dependent. These considerations have led us to propose the model, depicted in Scheme 2, in which there is ATP-dependent Ca<sup>2+</sup> binding to the myofibrils, the principal cytosolic Ca<sup>2+</sup>-buffer. In the model, a first Ca<sup>2+</sup> is bound, followed by ATP which effectively raises the affinity of a second Ca<sup>2+</sup> binding from low to high. The second Ca<sup>2+</sup> is then bound. Hydrolysis of the ATP (with a rate constant of 65s<sup>-1</sup> [18]) causes the second Ca<sup>2+</sup> binding site to revert to its low affinity state thereby enabling the myofibrils to relax through rapid release of Ca<sup>2+</sup>.

### Estimation of Ca<sup>2+</sup>-buffering in the intact heart

The new kinetic model of Ca<sup>2+</sup>-buffering was constrained to fit our data for the <sup>19</sup>F-NMR measurement of [Ca<sup>2+</sup>]<sub>i</sub> in the Langendorff-perfused ferret heart as well as the *in vitro* data for the [ATP] dependence of the myofibrillar ATPase [15] (see Figures 3 and 4). Under these constraints, a value was derived for the concentration of the myofibrillar Ca<sup>2+</sup> binding sites of 58μM with half activation of the ATPase at 580nM. Solaro *et al.* [29] estimated the concentration of high affinity Ca<sup>2+</sup> specific binding sites in ventricular muscle to be ≈70μM, which is close to the value derived from our model.

To estimate the concentration and affinities of endogenous Ca<sup>2+</sup> buffers it was necessary to know how much Ca<sup>2+</sup> was released into the cytoplasm during each Ca<sup>2+</sup> transient. To allow for the possibility that the depolarization-induced Ca<sup>2+</sup> release may vary with the increased buffering imposed by loading a Ca<sup>2+</sup> indicator, a “Ca<sup>2+</sup> store” with internal concentration [Ca<sup>2+</sup>]<sub>o</sub> and a release dependent on the difference, [Ca<sup>2+</sup>]<sub>o</sub> - [Ca<sup>2+</sup>]<sub>i</sub>, was included in the

model as a mathematical device. For such a store, if the [Ca<sup>2+</sup>]<sub>o</sub> is close to [Ca<sup>2+</sup>]<sub>i</sub> then the driving force for Ca<sup>2+</sup> release will be small and the amount released will be highly dependent on [Ca<sup>2+</sup>]<sub>i</sub> and therefore on the presence of Ca<sup>2+</sup> indicators if they perturb the [Ca<sup>2+</sup>]<sub>i</sub>. However, if the [Ca<sup>2+</sup>]<sub>o</sub> is high relative to the [Ca<sup>2+</sup>]<sub>i</sub> then the driving force for release will be large and the amount of Ca<sup>2+</sup> released will be effectively independent of [Ca<sup>2+</sup>]<sub>i</sub>. In solutions to our model the amount of Ca<sup>2+</sup> mobilized remained constant, 44μM for the Ca-ATP-Ca model, which suggests that there is no increase in mobilized Ca<sup>2+</sup> induced by the indicator. This prediction is consistent with the recent estimation of the concentration of free Ca<sup>2+</sup> in the sarcoplasmic reticulum of ≈700μM buffered by 14mM binding sites with K<sub>d</sub> ≈ 640μM [30]. It is also in agreement with the study from Adachi-Akahane *et al.* [31] who showed that the amount of Ca<sup>2+</sup> released from the sarcoplasmic reticulum was unaffected by increasing the cytosolic Ca<sup>2+</sup> buffering up to 16mM (2mM Fura-2 plus 14mM EGTA). Estimates from the model of 40–44μM mobilized Ca<sup>2+</sup> are very similar to the recent estimates of Ca<sup>2+</sup> release in ferret ventricular myocytes of 30–60μM [32], but are less than those estimated in many previous studies (typically 100–130μM: [7,10,33]). It is possible that the earlier studies overestimated the release of Ca<sup>2+</sup> because they were assumed much higher values for Ca<sup>2+</sup> buffering than were calculated in our model. It is also possible that species variations, which are known to contribute to differences in Ca<sup>2+</sup>-handling in the heart, may provide part of the explanation [34].

### Endogenous buffers

The Ca-ATP-Ca model was able to fit our experimental data to within experimental error without the need to include any buffering other than the myofibrils. However, this does not exclude the possibility that other buffers present could contribute to the total. The K<sub>d</sub> values for the four calmodulin Ca<sup>2+</sup> binding sites, when measured under *in vivo* conditions, all have values well below 100nM and slow dissociation rates [5]; they will therefore not contribute significantly to Ca<sup>2+</sup>-buffering. This is consistent with calmodulin having a control function that depends on the “average” and not the cycling [Ca<sup>2+</sup>]<sub>i</sub>. The K<sub>d</sub> for the sarcolemmal Ca<sup>2+</sup> binding sites has been estimated to be 180nM [9]. However, the voltage dependence of this Ca<sup>2+</sup> binding site (i.e. depolarization causes a reduction in affinity; which would result in release of Ca<sup>2+</sup> rather than binding of Ca<sup>2+</sup> during the transient, [35]) makes this site unlikely to contribute to Ca<sup>2+</sup>-buffering. It has recently been shown that Ca<sup>2+</sup> re-uptake by the sarcoplasmic reticulum (SR) could be best described by a process that binds Ca<sup>2+</sup> with a Hill coefficient

of 2 and is half-saturated when  $[Ca^{2+}] = 500nM$  [36]. These parameters would enable the SR to make a significant contribution to  $Ca^{2+}$ -buffering during the cardiac  $Ca^{2+}$  transient. However, the SR also releases  $Ca^{2+}$  during the ascending phase of the transient and its  $Ca^{2+}$  binding may follow that of the sarcolemma. The estimated concentration of SR  $Ca^{2+}$  uptake sites of  $19\mu M$  [10] could be included within that estimated here.

In the present study the approximation that all indicators were loaded to the same concentration of  $120\mu M$  is a potential source of inaccuracy in the calculation of the endogenous buffering present in the heart. However, as  $120\mu M$  is two to three times the estimated concentration of endogenous buffers any errors would occur in the estimation of the total concentration of  $Ca^{2+}$  binding sites but have little effect on the estimated affinity of those sites.

### Effect of loading $Ca^{2+}$ -indicators on cardiac $Ca^{2+}$ transients

A useful prediction of the model is the extent of perturbation of the  $Ca^{2+}$  transient expected on introducing additional exogenous buffers, such as  $Ca^{2+}$  indicators. For the simplest model, i.e. containing only the myofibrils, as little as  $30\mu M$  of an indicator with a  $K_d$  of  $220nM$  would cause more than 50% reduction in the magnitude of the  $Ca^{2+}$  transient (see Figure 8). In most studies where  $[Ca^{2+}]_i$  is measured using spectroscopic  $Ca^{2+}$  indicators there has been no estimation of the concentration of indicator present in the cytosol although it appears that the concentrations used range from 30 to  $900\mu M$  [4]. As well as causing significant perturbations of the  $[Ca^{2+}]_i$ , such concentrations of added indicators will also slow the transients (e.g. see [27]) and therefore complicate kinetic analysis of  $Ca^{2+}$  handling in the heart. Significant perturbation of  $Ca^{2+}$  transients caused by loading  $Ca^{2+}$  indicators is not limited to cardiac muscle (see Zhou and Neher [37] who noted similar perturbations in chromaffin cells).

### The Hill coefficients of the myofibrillar ATPase and $^{45}Ca$ binding

A conventional model of cardiac myofibrillar ATPase activity, i.e. one which included a single  $Ca^{2+}$ -binding site and an ATP-binding step, was unable to reproduce our experimental data (see Figure 4). Conversely, a model that included ATP-dependent cooperative  $Ca^{2+}$  binding to the myofilaments was able to reproduce our experimental data. Furthermore, this model was able to predict values for the  $Ca^{2+}$  dependency of the myofibrillar ATPase that closely agreed with the experimental data of Holroyde *et al.* [11] (see Figure 6).

The model presented here explains the increased cooperativity of  $^{45}Ca$  binding in the presence of ATP although this is not accompanied by a clear increase in numbers of  $Ca^{2+}$  bound. In the absence of ATP the species formed is  $M Ca_2$ , where M is a dimeric unit and the affinities show no cooperativity. In the presence of ATP the species formed ( $M Ca_2 ATP$ ) has high  $Ca^{2+}$  cooperativity but again only one  $Ca^{2+}$  per sub unit. The results in this paper introduce an unexpected mode of interaction between sub units of the myofibril to answer the question of how the apparent cooperativity of  $Ca^{2+}$  activation could arise. It could arise either at the  $Ca^{2+}$  binding level or, as previously argued, after substrate binding. If it arose after substrate binding, e.g. via the interaction of two activated actomyosin sub units, then there would be no need to invoke a second  $Ca^{2+}$  binding site per ATPase. It would then be expected that, in addition to the apparent Hill coefficient for the  $[Ca^{2+}]$  dependency of the ATPase being greater than 1 (see Figure 2), the Hill coefficient for the  $[ATP]$  dependence of the ATPase activity would also be greater than 1. The Hill coefficient for  $[ATP]$ , however, is unity (see Figure 4), so we can exclude the possibility that any of the apparent higher order for  $Ca^{2+}$  dependency is due to positive cooperativity between ATPases or with cross bridges. The present model requires that cardiac myofibrils have a second  $Ca^{2+}$  binding site on an interacting sub unit with an apparent affinity that is modulated by ATP binding. The situation may also be viewed as the binding of ATP reduces the affinity of interacting sub units to bind the first  $Ca^{2+}$  and increases that for the second. Importantly, only one ATP is hydrolysed by the two interacting sub units.

The situation is similar in the cooperative  $Ca^{2+}$ -binding by, and  $Ca^{2+}$ -activation of, myofibrils from skeletal muscle [38]. These have one major difference from the cardiac myofibrils; skeletal muscle troponin-C is known to have two  $Ca^{2+}$ -specific binding sites with dissociation rates in the physiologically relevant range, whereas, cardiac troponin-C has only one [9,11,12].

## Acknowledgements

AAG is a British Heart Foundation Senior Research Fellow (FS/97026) and JIV a British Heart Foundation Basic Science Lecturer (BS/9502). ATPase  $\text{Ca}^{2+}$  dependency data (Figures 1 and 6) used with permission of Dr. J. Potter and the ATP dependency (Figure 4) with permission of Dr. W. Jacobus.

## References

- Chapman, R. A. (1983) Control of cardiac contractility at the cellular level. *Am J Physiol* **245**:H535–52
- Kirschenlohr, H. L., Grace, A. A., Vandenberg, J. I., Metcalfe, J. C. and Smith, G. A. (2000) Estimation of systolic and diastolic free intracellular  $\text{Ca}^{2+}$  by titration of  $\text{Ca}^{2+}$  buffering in the ferret heart. *Biochem J* **346 Pt 2**:385–91 (**Paper I** in this series)
- Wier, W. G. (1990) Cytoplasmic  $[\text{Ca}^{2+}]$  in mammalian ventricle: dynamic control by cellular processes. *Annu Rev Physiol* **52**:467–85
- Noble, D. and Powell, T. (1991) The slowing of  $\text{Ca}^{2+}$  signals by  $\text{Ca}^{2+}$  indicators in cardiac muscle. *Proc R Soc Lond B Biol Sci* **246**:167–72
- Johnson, J. D., Snyder, C., Walsh, M. and Flynn, M. (1996) Effects of myosin light chain kinase and peptides on  $\text{Ca}^{2+}$  exchange with the N- and C-terminal  $\text{Ca}^{2+}$  binding sites of calmodulin. *J Biol Chem* **271**:761–7
- Pierce, G. N., Philipson, K. D. and Langer, G. A. (1985) Passive calcium-buffering capacity of a rabbit ventricular homogenate preparation. *Am J Physiol* **249**:C248–55
- Hove-Madsen, L. and Bers, D. M. (1993) Passive  $\text{Ca}^{2+}$  buffering and SR  $\text{Ca}^{2+}$  uptake in permeabilized rabbit ventricular myocytes. *Am J Physiol* **264**:C677–86
- Berlin, J. R., Bassani, J. W. and Bers, D. M. (1994) Intrinsic cytosolic calcium buffering properties of single rat cardiac myocytes. *Biophys J* **67**:1775–87
- Bers, D. (1991) Excitation contraction coupling and cardiac contractile force. *Kluwer Academic Publishers, Dordrecht*
- Fabiato, A. (1983) Calcium-induced release of calcium from the cardiac sarcoplasmic reticulum. *Am J Physiol* **245**:C1–14
- Holroyde, M. J., Robertson, S. P., Johnson, J. D., Solaro, R. J. and Potter, J. D. (1980) The calcium and magnesium binding sites on cardiac troponin and their role in the regulation of myofibrillar adenosine triphosphatase. *J Biol Chem* **255**:11688–93
- Pan, B.-S., and R. J. Solaro. 1987. Calcium-binding properties of troponin-C in detergent-skinned heart muscle fibers. *J Biol Chem* **262**:7839–49
- Morimoto, S. and Ohtsuki, I. (1994)  $\text{Ca}^{2+}$  binding to cardiac troponin-C in the myofilament lattice and its relation to the myofibrillar ATPase activity. *Eur J Biochem* **226**:597–602
- Harding, D. P., Smith, G. A., Metcalfe, J. C., Morris, P. G. and Kirschenlohr, H. L. (1993) Resting and end-diastolic  $[\text{Ca}^{2+}]_i$  measurements in the Langendorff-perfused ferret heart loaded with a  $^{19}\text{F}$ -NMR indicator. *Magn Reson Med* **29**:605–15
- Krause, S. M., and W. E. Jacobus. 1992. specific enhancement of the cardiac myofibrillar ATPase by bound creatine kinase. *J Biol Chem* **267**:2480–6
- Marban, E., Kusuoka, H., Yue, D. T., Weisfeldt, M. L. and Wier, W. G. (1986) Maximal  $\text{Ca}^{2+}$ -activated force elicited by tetanization of ferret papillary muscle and whole heart: mechanism and characteristics of steady contractile activation in intact myocardium. *Circ Res* **59**:262–9
- Johnson, J. D., Nakkula, R. J., Vasulka, C. and Smillie, L. B. (1994) Modulation of  $\text{Ca}^{2+}$  exchange with the  $\text{Ca}^{2+}$ -specific regulatory sites of troponin-C. *J Biol Chem* **269**:8919–23
- Taylor, R. S., and A. G. Weeds. 1976. The magnesium-ion-dependent adenosine triphosphatase of bovine cardiac myosin and its subfragment-1. *Biochem J* **159**:301–15
- Tobacman, L. S. and Sawyer, D. (1990) Calcium binds cooperatively to the regulatory sites of the cardiac thin-filament. *J Biol Chem* **265**:931–9
- Arata, T., Mukohata, Y. and Tonomura, Y. (1977) Structure and function of the two heads of the myosin molecule. VI. ATP hydrolysis, shortening, and tension development of myofibrils. *J Biochem (Tokyo)* **82**:801–12
- Marston, S. B. and Taylor, E. W. (1980) Comparison of the myosin and actomyosin ATPase mechanisms of the four types of vertebrate muscles. *J Mol Biol* **139**:573–600
- Morris, P. G., Allen, D. G. and Orchard, C. H. (1985) High-time-resolution  $^{31}\text{P}$  NMR studies of the perfused ferret heart. *Adv Myocardiol* **5**:27–37
- Kirschenlohr, H. L., Metcalfe, J. C., Morris, P. G., Rodrigo, G. C. and Smith, G. A. (1988)  $\text{Ca}^{2+}$  transient,  $\text{Mg}^{2+}$ , and pH measurements in the cardiac cycle by  $^{19}\text{F}$ -NMR. *Proc Natl Acad Sci USA* **85**:9017–21
- McAuliffe, J. J., Gao, L. Z. and Solaro, R. J. (1990) Changes in myofibrillar activation and troponin-C  $\text{Ca}^{2+}$  binding associated with troponin T isoform switching in developing rabbit heart. *Circ Res* **66**:1204–16
- Kirschenlohr, H. L., Grace, A. A., Clarke, S. D., Shachar-Hill, Y., Metcalfe, J. C., Morris, P. G. and Smith, G. A. (1993) Calcium measurements with a new high-affinity NMR indicator in the isolated perfused heart. *Biochem J* **293**:407–11
- Metcalfe, J. C., Hesketh, T. R. and Smith, G. A. (1985) Free cytosolic  $\text{Ca}^{2+}$  measurements with fluorine labelled indicators using  $^{19}\text{F}$ -NMR. *Cell Calcium* **6**:183–95
- Balke, C. W., Egan, T. M. and Wier, W. G. (1994) Processes that remove calcium from the cytoplasm during excitation-contraction coupling in intact rat heart cells. *J Physiol (Lond)* **474**:447–62
- Bassani, R. A., Bassani, J. W. and Bers, D. M. (1994) Relaxation in ferret ventricular myocytes: unusual interplay among calcium transport systems. *J Physiol (Lond)* **476**:295–308
- Solaro, R. J., Wise, R. M., Shiner, J. S. and Briggs, F. N. (1974) Calcium requirements for cardiac myofibrillar activation. *Circ Res* **34**:525–30
- Shannon, T. R. and Bers, D. M. (1997) Assessment of intra-SR free  $[\text{Ca}^{2+}]$  and buffering in rat heart. *Biophys J* **73**:1524–31
- Adachi-Akahane, S., Cleemann, L. and Morad, M. (1996) Cross-signaling between L-type  $\text{Ca}^{2+}$  channels and ryanodine receptors in rat ventricular myocytes. *J Gen Physiol* **108**:435–54

32. Bassani, R. A., Bassani, J. W. and Bers, D. M. (1995) Relaxation in ferret ventricular myocytes: role of the sarcolemmal Ca ATPase. *Pflugers Arch* **430**:573–8
33. Sipido, K. R. and Wier, W. G. (1991) Flux of Ca<sup>2+</sup> across the sarcoplasmic reticulum of guinea-pig cardiac cells during excitation-contraction coupling. *J Physiol (Lond)* **435**:605–30
34. Bassani, J. W., Bassani, R. A. and Bers, D. M. (1994) Relaxation in rabbit and rat cardiac cells: species-dependent differences in cellular mechanisms. *J Physiol (Lond)* **476**:279–93
35. Bers, D. M., Allen, L. A. and Kim, Y. (1986) Calcium binding to cardiac sarcolemmal vesicles: potential role as a modifier of contraction. *Am J Physiol* **251**:C861–71
36. Bers, D. M. and Berlin, J. R. (1995) Kinetics of [Ca<sup>2+</sup>]<sub>i</sub> decline in cardiac myocytes depend on peak [Ca<sup>2+</sup>]<sub>i</sub>. *Am J Physiol* **268**:C271–7
37. Zhou, Z. and Neher, E. (1993) Mobile and immobile calcium buffers in bovine adrenal chromaffin cells. *J Physiol (Lond)* **469**:245–73
38. Brandt, P. W., Cox, R. N., Kawai, M. and Robinson, T. (1982) Effect of cross-bridge kinetics on apparent Ca<sup>2+</sup> sensitivity. *J Gen Physiol* **79**:997–1016
-